Adaptive dielectric liquid lens

Hongwen Ren, Haiqing Xianyu, Su Xu, and Shin-Tson Wu

College of Optics and Photonics, University of Central Florida, Orlando, Florida 32816, USA
swu@mail.ucf.edu

Abstract: A tunable-focus liquid lens using dielectrophoretic effect is demonstrated. When a voltage is applied to a dielectric liquid droplet, the generated electric field inside the droplet is inhomogeneous. As a result, the liquid bears a dielectric force and its surface profile can be reshaped which causes the focal length to change. Adaptive lenses with different apertures are fabricated and their performances evaluated. In comparison to the patterned-electrode liquid lenses, our lens uses continuous electrode which is much simpler for fabrication.

OCIS codes: (010.1080) adaptive optics; (220.3630) lens; (230.2090) electro-optical devices.

References and links

1. M. Ye and S. Sato, "Optical properties of liquid crystal lens of any size," Jpn. J. Appl. Phys. **41**, L571-L573 (2002).
2. B. Wang, M. Ye, M. Honma, T. Nose, and S. Sato, "Liquid crystal lens with spherical electrode," Jpn. J. Appl. Phys. **41**, L1232-L1233 (2002).
3. H. Ren Y. H. Fan, S. Gauza, and S. T. Wu, "Tunable-focus flat liquid crystal spherical lens," Appl. Phys. Lett. **84**, 4789-4791 (2004).
4. X. Wang, H. Dai, and K Xu, "Tunable reflective lens array based on liquid crystal on silicon," Opt. Express **13**, 352-357 (2005).
5. J. S. Patel and K. Rastani, "Electrically controlled polarization-independent liquid-crystal Fresnel lens arrays," Opt. Lett. **16**, 532-534 (1991).
6. G. Li, P. Valley, M. S. Giridhar, D. L. Mathine, G. Meredith, J. N. Haddock, B. Kippelen, and N. Peyghambarian, "Large-aperture switchable thin diffractive lens with interleaved electrode patterns," Appl. Phys. Lett. **89**, 141120 (2006).
7. N. Chronis, G. L. Liu, K. H. Jeong, and L. P. Lee, "Tunable liquid-filled microlens array integrated with microfluidic network," Opt. Express **11**, 2370-2378 (2003).
8. K. S. Hong, J. Wang, A. Sharonov, D. Chandra, J. Aizenberg, and S. Yang, "Tunable microfluidic optical devices with an integrated microlens array," J. Micromech. Microeng. **16**, 1660-1666 (2006).
9. J. Chen, W. Wang, J. Fang, and K. Varahramtan, "Variable-focusing microlens with microfluidic chip," J. Micromech. Microeng. **14**, 675-680 (2004).
10. H. Ren and S. T. Wu, "Variable-focus liquid lens," Opt. Express **15**, 5931-5936 (2007).
11. T. Krupenkin, S. Yang, and P. Mach, "Tunable liquid microlens," Appl. Phys. Lett**. 82**, 316-318 (2003).
12. S. Kuiper and B. H. W. Hendriks, "Variable-focus liquid lens for miniature cameras," Appl. Phys. Lett. **85**, 1128-1130 (2004).
13. M. Vallet, B. Berge, and L. Vovelle, "Electrowetting of water and aqueous solutions on poly (ethylene terephthalate) insulating films," Polymer **37**, 2465-2470 (1996).
14. C. C. Cheng and J. A. Yeh, "Dielectrically actuated liquid lens," Opt. Express **15**, 7140-7145 (2007).
15. H. Ren and S. T. Wu, "Tunable-focus liquid microlens array using dielectrophoretic effect," Opt. Express **16**, 2646-2652 (2008).
16. H. Ren, D. Fox, B. Wu, and S. T. Wu, "Liquid crystal lens with large focal length tunability and low operating voltage," Opt. Express **15**, 11328 (2007).
17. S. Gauza, H. Wang, C. H. Wen, S. T. Wu, A. J. Seed, and R. Dabrowski, "High birefringence isothiocyanato tolane liquid crystals," Jpn. J. Appl. Phys. Part 1, **42**, 3463-3466 (2003).
18. S. Gauza, C. H. Wen, S. T. Wu, N. Janarthanan, and C. S. Hsu, "Super high birefringence isothiocyanato biphenyl-bistolane liquid crystals," Jpn. J. Appl. Phys. **43**, 7634-7638 (2004).
19. J. D. Jackson, *Classical Electrodynamics* (Viley, New York, 1975), 2nd ed.

1 . Introduction

Lens is an important optical element for image processing, optical communication, machine vision, and camera applications. A lens made of glass, polymer or other clear solid materials

#96286 - $15.00 USD Received 16 May 2008; revised 23 Jul 2008; accepted 30 Aug 2008; published 8 Sep 2008

has a fixed focus because of the rigid surface profile. To change the focal length, a lens system which contains at least two lenses is necessary. In such a zoom lens system, the effective focal length is variable by mechanically adjusting the distance between the lenses along the optical axis. Such a lens system is usually bulky, complicated, and heavy. Therefore, it is highly desirable to develop an adaptive lens without mechanical moving parts.

Several adaptive lenses have been developed. Based on operation mechanisms, they can be roughly classified into two categories: liquid crystal (LC) lens [1-6] and liquid lens [7-15]. In a LC lens, by applying an inhomogeneous electric field the LC molecules can be reoriented to produce a gradient refractive index profile across the lens aperture. The focal length of a LC lens is related to lens radius (r), refractive index difference between the lens center and boarder (δn), and LC layer thickness (d) as $f \sim r^2/(2d \cdot \delta n)$ [16]. To obtain a short focal length, we could increase $d \cdot \delta n$ or reduce the lens aperture. A high birefringence LC has Δn~0.4 [17]. Some ultra-high Δn (>0.6) LCs exist [18], but their viscosity is too high to be practically useful. On the other hand, increasing d helps to reduce focal length, but it is unfavorable from the viewpoint of response time. Therefore, LC is more suitable for microlens [4] and zoned lens [5,6] rather than a large-aperture lens.

An adaptive liquid lens focuses light based on the shape change. Its optical path-length change is much larger than that of a LC lens. Thus, it is suitable for a large aperture lens with a wide dynamic range. Three kinds of liquid lenses, e.g., membrane lens, electro-wetting lens, and dielectric lens, have been developed. Different from an elastic membrane lens whose shape change is manipulated mechanically [7-10], both electro-wetting lens [11-13] and dielectric lens [14-15] use an external voltage to tune the focal length. These two types of lenses have similar features, e.g., there are two immiscible liquids in the lens cell; one liquid forms a droplet on one inner substrate surface and the other liquid fills the surrounding space of the droplet. In contrast to an electro-wetting lens, the two liquids employed in the dielectric lens are nonconductive but with different dielectric constants. Dielectric lenses are very stable and can bear a high operating voltage. Moreover, their power consumption is low because of little heat generation. As a result, no micro-bubbles appear during focus change. To drive the dielectric lens, the applied electric field should be inhomogeneous in order to generate dielectric force. To do so, the electrode of the dielectric lens is etched with holes or rings. Patterning electrode definitely increases the complexity of device fabrication.

In this paper, we demonstrate an adaptive dielectric lens using continuous flat electrodes. Through our theoretical analyses, we find that when a voltage is applied to a dielectric liquid droplet the generated electric field inside the droplet is inhomogeneous. Therefore, the droplet bears a dielectric force which reshapes the droplet surface and alters the focus. We have fabricated several dielectric lenses with different apertures and evaluated their performances.

2. Device structure and theoretical analysis

Figure 1(a) depicts the side-view structure of the lens cell. From top to bottom, it consists of a planar glass plate, indium tin oxide (ITO) electrode, liquid-1, liquid-2, a polymer layer, ITO electrode, and a planar glass plate. Both top and bottom glass plates have ITO electrode but only bottom plate has a thin polymer layer. The two liquids are immiscible but with different dielectric constants. Liquid-2 has a low dielectric constant; it forms a droplet on the bottom substrate surface. On the other hand, liquid-1 has a high dielectric constant and it fills the surrounding space. In the relaxed state, the curvature of the droplet is minimal. When a voltage is applied, the two liquids experience an electric field. For the droplet, the electric field within it can be expressed as:

$$E_t = \frac{V \big/ \varepsilon_2}{\frac{t}{\varepsilon_2} + \frac{d-t}{\varepsilon_1} + \frac{d_P}{\varepsilon_P}}, \tag{1}$$

#96286 - $15.00 USD Received 16 May 2008; revised 23 Jul 2008; accepted 30 Aug 2008; published 8 Sep 2008

where ε_1, ε_2, and ε_p represent the dielectric constant of liquid-1, liquid-2, and polymer layer, respectively; d is the cell gap, d_p is the thickness of polymer layer, and t is the height of liquid-2 from the polymer surface to the curved surface of the droplet along vertical direction. Some parameters are shown in Fig. 1(b).

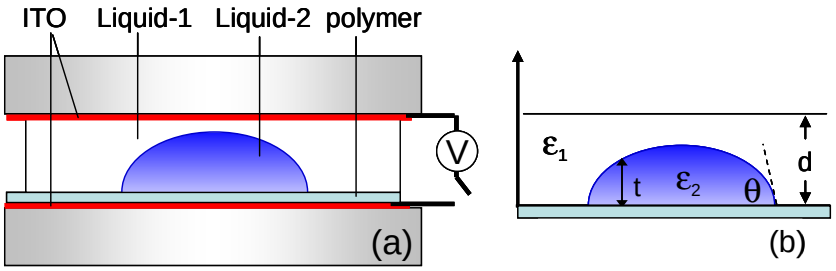

Fig. 1. (a) Side-view structure of the lens cell and (b) definition of the involved parameters.

In Eq. (1), the influence of d_p/ε_p to E_t is negligible if the coated polymer layer is very thin, i.e., $d_p \to 0$. In this case, the electric field E_t near the droplet border can be approximated as

$$E_{t\to 0} = \frac{V\varepsilon_1}{d\varepsilon_2}. \tag{2}$$

If the apex distance of the droplet is approaching the cell gap ($t \to d$), then the electric field E_t at the apex position of the droplet can be approximated as

$$E_{t\to d} = \frac{V}{d}. \tag{3}$$

From Eqs. (2) and (3), the electric filed at the border is $\varepsilon_1/\varepsilon_2$ times stronger than that at the apex position. Because the surface of the droplet changes continuously, the electric field has a gradient distribution.

According to Kelvin theory [19], when the droplet experiences such an electric field a dielectric force exerting to the curved surface is generated. The dielectric force is expressed as

$$\vec{F} = \frac{\varepsilon_0}{2}(\varepsilon_1 - \varepsilon_2)\nabla(E \bullet E), \tag{4}$$

where ε_0, ε_1 and ε_2 represent the permittivity of free space, liquid-1, and liquid-2, respectively, and E denotes the electric field on the curved droplet surface. From Eq. (4), the difference of ε_1 and ε_2 and the electric field gradient play key roles to the dielectric force. If ε_1 is equal to ε_2, then the net force is zero. Also, the force changes sign depending on whether the droplet's dielectric constant is larger or smaller than that of liquid-1.

When the dielectric force is strong enough, liquid-1 has the tendency to move toward the strong electric field region, while liquid-2 toward the weak electric field region. As a result, the surface profile of the droplet is reshaped. From Eq. (1), the droplet has the tendency to contract if the electric filed is above the threshold. Equations (2) and (3) imply that when the droplet is highly contracted the apex distance is almost the same as the cell gap. Since the shape of the droplet is axially symmetric, the droplet exhibits a lens property. The focal length of the droplet has following form [12]:

$$f^3 = \frac{3V_d}{\pi(1-\cos\theta)(2-\cos^2\theta-\cos\theta)(n_2-n_1)^3}, \tag{5}$$

where V_d is the volume of the droplet, n_1 and n_2 are the refractive indices of liquid-1 and liquid-2, and θ is the contact angle. As the contact angle changes, the shape of the liquid droplet changes which, in turn, results in a different focal length.

#96286 - $15.00 USD Received 16 May 2008; revised 23 Jul 2008; accepted 30 Aug 2008; published 8 Sep 2008

3. Experiment

To prepare a lens cell as sketched in Fig. 1(a), we coated the ITO side of the bottom glass plate with a polymer layer (d_p~0.8 μm and ε_P~4). This polymer layer serves for two purposes: to lubricate the substrate surface and to enhance the contact angle of the droplet. Without this layer, the droplet on the ITO surface will have a strong friction and is not easy to reshape. For experimental demonstration, we chose two liquids with their parameters listed in Table 1. Liquid-2 was used as the droplets and liquid-1 as the surrounding media. Another ITO glass plate was used as top substrate to seal the cell. The cell gap was controlled at d~110 μm.

Table 1. Key parameters of liquid-1 and liquid-2. The unit of surface tension is mN/m and density is g/cm^3.

	Dielectric Constant	Refractive Index @ 589 nm	Abbe Number	Surface Tension	Density	Color
Liquid-1	47	1.472	59	63	1.25	Clear
Liquid-2	5	1.673	22	50	1.26	Clear

4. Results

For a small lens, we used an optical microscope to evaluate its imaging performance. The cell was placed on the microscope stage which can travel in vertical direction. Firstly, we observed the two-dimensional (2D) focal spot of one liquid droplet (diameter ~230 μm). At V=0, we focused on the droplet's surface and the image is shown in Fig. 2(a). The droplet is highly circular and has a clear border with the surrounded liquid. To easily see the focus change, we intentionally adjusted the position of the lens cell such that a large focal spot is observed, as shown in Fig. 2(b). In this state the border of the large spot presents red color which implies it is an inside focus. When a voltage of 90 V_{rms} (~300 Hz) was applied to the electrode, the spot size was decreased significantly, as shown in Fig. 2(c). The border of the spot presents blue color which means it is an outside focus. The results shown in Figs. 2(b) and 2(c) indicate that the focal length of the droplet is electrically tunable. The axial color change of the spot is due to the color dispersion of the liquid materials. Such color dispersion is a common issue even in a conventional glass lens. From Fig. 2, light is highly focused at the center area and no noise occurs in the dark ground. Such a focusing ability of the liquid lens is as good as a conventional glass lens.

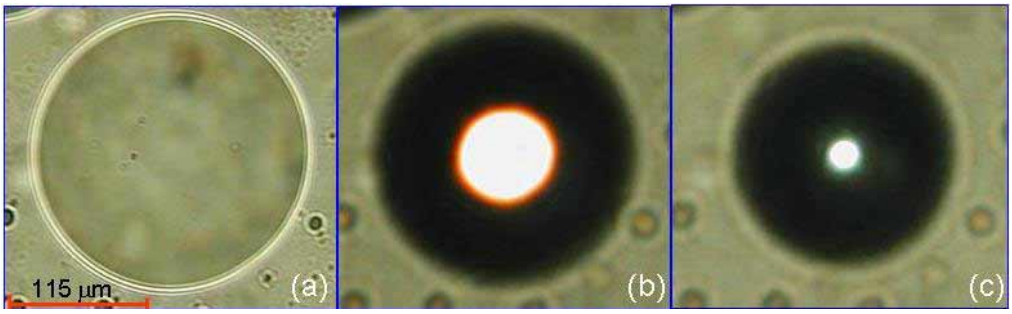

Fig. 2. The 2D image of the lens cell at the position of (a) surface focus, (b) inside focus, and (c) outside focus.

Another method to evaluate the lens quality is to observe the image performance through the lens. Here we focused on two droplets with the same diameter of ~230 μm. To study the imaging performance, a small letter "5" was typed on a piece of transparency as an object. The object was placed under the lens cell. By adjusting the cell position, a clear image in the voltage-off state was observed in white light, as shown in Fig. 3(a). In contrast to the original

#96286 - $15.00 USD Received 16 May 2008; revised 23 Jul 2008; accepted 30 Aug 2008; published 8 Sep 2008

object, the image "5" is inverted. We then applied 60 V_{rms} to the lens cell and the image became blurry instantly due to the defocusing effect, as shown in Fig. 3(b). To restore the clarity, we translated the microscope stage in vertical direction while the voltage was still applied. The image after refocusing is shown in Fig. 3(c). It is still very clear except for the reduced size. Because the densities of the two liquids match well, the surface profile of the droplet is affected by the gravity effect. Very similar to an elastic membrane lens, if we mimic the liquid layer of the interface between the two liquids as an elastic membrane (the thickness is negligible), then the surface of each droplet mainly presents a parabolic shape. Therefore, the defocus, spherical aberration, and color dispersion are the main causes for any incurred image blurry.

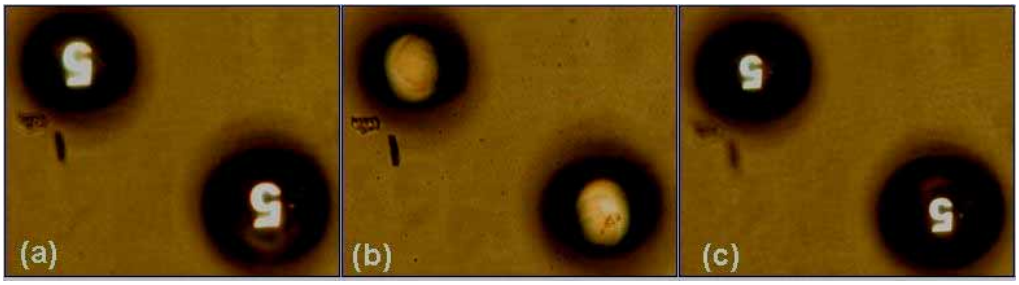

Fig. 3. Imaging properties of two liquid lenses at (a) V=0, (b) V=60 V_{rms}, and (c) refocused state.

To measure the focal length of the liquid droplet, we first adjusted the position of the lens cell so that we focused on the droplet surface, as shown in Fig. 2(a). Secondly, we adjusted the cell position vertically so that we saw a clear image, as shown in Fig 3(a). The distance that the cell traveled is the focal length of the lens. This method also applied to the lens cell with a voltage. The focal length of one lens shown in Fig. 3 was measured at different voltages. The voltage dependent focal length is plotted in Fig. 4. At V=0, the inherent focal length of the lens is f~620 μm. As the voltage increases, the focal length is gradually decreased. At V=90 V_{rms}, the focal length is decreased to ~500 μm.

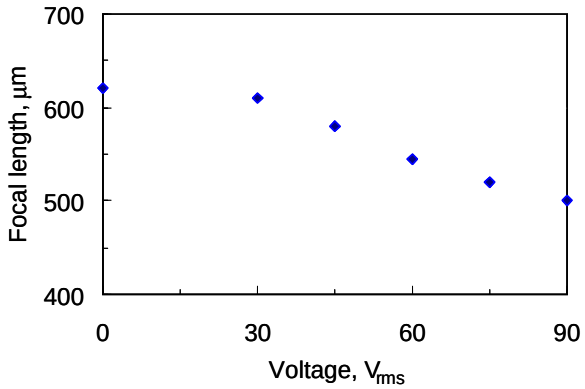

Fig. 4. The measured voltage-dependent focal length of a dielectric liquid lens with 230 μm diameter.

As the voltage increases, the focal length of the liquid lens should decrease further. However, a too high voltage may cause two problems: 1) the surface profile of the lens could be deformed severely, and 2) the droplet could touch the opposite substrate surface. The former will degrade the lens performance and the latter will damage the droplet's geometric structure.

#96286 - $15.00 USD Received 16 May 2008; revised 23 Jul 2008; accepted 30 Aug 2008; published 8 Sep 2008

When the lens aperture shrinks, the apex distance has to change. Based on the parameters of the lens cell listed in Table 1, the measured focal length *f*~620 μm, and lens aperture ~230 μm, we calculated the apex distance at V=0 to be ~77.6 μm using the Code-V software. Subsequently, the volume of the droplet was calculated to be ~0.0006π mm^3. In addition, from Eq. (5) we can estimate the contact angle from the measured focal length. At V=0, the contact angle was found to be θ~68°. At V=90 V_{rms}, the diameter of the droplet shrinks to 198 μm (see Fig. 2(c)). Because the volume of the droplet does not change, the apex distance is increased to ~90 μm and contact angle is also increased to 85°. Due to the thick cell gap (d~110 μm), the contracted droplet does not touch the top substrate. Therefore, the capillary effect will not occur and this voltage is still very safe to the liquid droplets.

Based on the parameters of the employed liquid materials, the performance of the liquid lens can be further estimated using Code-V software. Suppose the droplet presents a parabolic shape (conic constant k=-1) and three wavelengths (656, 589, and 486 nm) with weighting ratios 1:1:1 are chosen, then at V=0 the composite root-mean-square (RMS) wavefront aberration is 0.163 waves (at λ=546.3 nm). In this case, the strehl ratio is 0.350. At V=90 V_{rms}, the composite RMS wavefront aberration is 0.147 waves (at λ=546.3 nm) and the strehl ratio is 0.427. The performance is slightly improved because of the decreased lens aperture. In most cases, the lens works under white light ambient. Thus, color aberration is an important parameter to evaluate the lens quality. Based on the lens parameters, we also calculated the color aberrations of the lens. The calculated aberrations along axial and lateral positions are 0.006282 mm and -0.000014 mm at V=0, and 0.005434 mm and 0.000035 mm at V=90 V_{rms}, respectively. Because the liquid-2 we employed is very dispersive (its Abbe number is ~22), to correct the color aberration we could substitute it by another liquid with a large Abbe number while keeping other parameters unchanged.

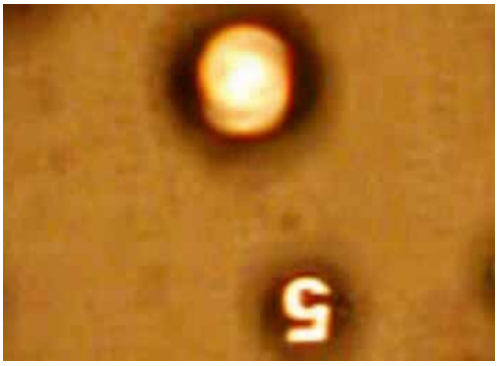

Fig. 5. Two different liquid lenses driven from focus (defocused) state to defocused (focus) states. (Media 1).

Response time is important for an adaptive lens during focus change. Undoubtedly, the contracting speed of the droplet is mainly dependent on the dielectric force and the relaxing speed is dependent on the viscosity of the liquids and the related interfacial tensions. Theoretical calculation of the response speed is rather difficult because the interface tensions of the liquid-liquid and liquid-substrate are complicated. Thus, we measured the response speed experimentally. To measure the contracting as well as the relaxing speed, we applied a square voltage burst at ~45 V_{rms} (f=300 Hz) to the lens cell. Different from Fig. 3(a), we chose two liquid droplets but with different diameters for the active driving. At V=0 the droplet (bottom) with diameters of ~230 μm was in focus and a clear image "5" was observed. At the same focused position, a larger droplet (top) with ~300 μm diameter was in a larger defocused state, so the image was very blurry. To visually observe the tunable state and the response speed, a movie for tuning the two lenses was taken, as shown in Fig. 5. When the smaller

#96286 - $15.00 USD Received 16 May 2008; revised 23 Jul 2008; accepted 30 Aug 2008; published 8 Sep 2008

droplet was defocused, the larger droplet was in focus and a clear image "5" was observed. The contracting speed of the two lenses is almost the same (~200 ms), but their relaxing speed is different. It is ~ 200 ms for the smaller lens and ~300 ms for the larger lens. In comparison with previous dielectric lenses [14,15], the measured response time is about the same.

From Fig. 1, the aperture of the droplet can be scaled up to several millimeters while still maintaining a spherical-like shape. A larger droplet will increase the apex distance and, thus, requires a thicker cell gap. As a result, the operating voltage will be higher. As a compromise, our lens is more suitable for microlens and microlens array.

In our experiments, both liquids have almost the same density and the droplet is firmly anchored to the inner bottom substrate surface due to the adhesive force. As a result, the gravity effect on the droplet shape is negligible and the position of the droplet is stable even the lens is placed in vertical direction. Therefore, the lens structure is insensitive to shocks and vibrations. Because the surface profile of the liquid lens is only controlled by the surface tension, the formed liquid surface is very smooth. Such a liquid lens usually provides a reasonable resolution before the surface shape is severely deformed by the dielectric force.

5. Conclusion

An adaptive liquid lens based on the dielectrophoretic effect is demonstrated. In our lens cell, the liquid droplet itself has the ability to convert a homogeneous electric field to an inhomogeneous one. This effect permits a continuous electrode be used directly for the lens cell. Owing to the inhomogeneous electric field, the generated dielectric force can reshape the surface profile of the droplet and change its focal length. In comparison to electrode-patterned liquid lenses, our lens has the advantages in easy fabrication and simple structure. Moreover, the surface profile of our liquid lens will not be distorted severely due to the smooth gradient of the electric field across the droplet surface. Therefore, such a liquid lens can provide a high image quality.

Acknowledgment

The authors are indebted to Meizi Jiao for the technical assistance.

#96286 - $15.00 USD Received 16 May 2008; revised 23 Jul 2008; accepted 30 Aug 2008; published 8 Sep 2008